RESEARCH ARTICLE

Figures and figure supplements

A novel monomeric amyloid β-activated signaling pathway regulates brain development via inhibition of microglia

Hyo Jun Kwon *et al*.

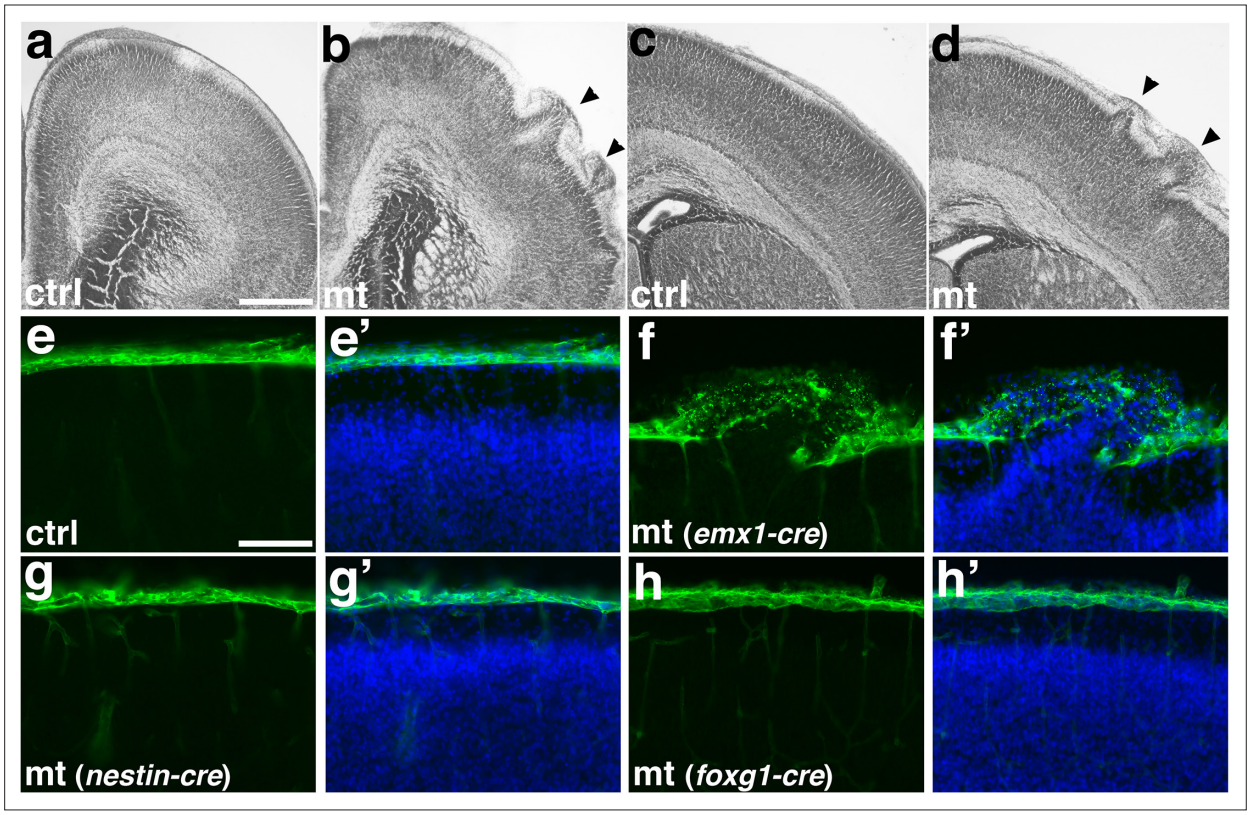

Figure 1. Deletion of *Ric8a* using *Emx1-Cre* results in cortical ectopia due to non-neural deficits. (**a–d**) Nissl staining of control (ctrl, (**a**)&**c**) and mutant mt, (**b**&**d**) anterior motor (**a–b**) and posterior somatosensory (**c–d**) cortex at P0. (**e-e'**) Laminin (LN, in green) and nuclear (DAPI, in blue) staining of control cortices at P0. A continuous basement membrane is observed at the pia, beneath which cells are well organized in the cortical wall. (**f-f'**) Staining of *Ric8a:Emx1-Cre* mutant cortices at P0. Basement membrane breach and neuronal ectopia are observed following *Ric8a* deletion by *Emx1-Cre*, a *Cre* line expressed in cortical radial glial progenitors beginning at E10.5. (**g-g'**) Staining of *Ric8a:Nestin-Cre* mutant cortices at P0. No obvious basement membrane breach or neuronal ectopia is observed following *Ric8a* deletion by *Nestin-Cre*, a *Cre* line expressed in cortical progenitors beginning around E12.5. (**h-h'**) Staining of *Ric8a:Foxg1-Cre* mutant cortices at P0. No obvious basement membrane breach or neuronal ectopia is observed following *Ric8a* deletion by *Foxg1-Cre*, a *Cre* line expressed in forebrain neural progenitors from E9.0. Scale bars, 640 μm for (**a–b**), 400 μm for (**c–d**), and 100 μm for (**e-h'**).

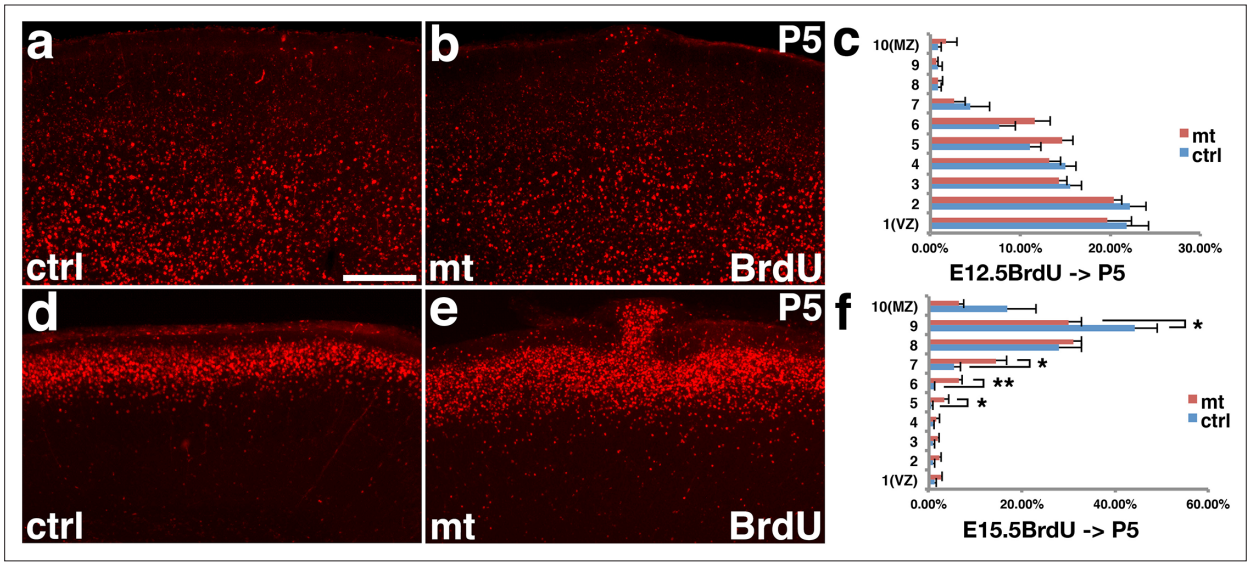

Figure 1—figure supplement 1. Birth-dating of early and late-born neurons in *Ric8a:Emx1-Cre* mutant cortices. (**a–c**) BrdU (in red) staining in control (**a**) and mutant (**b**) cortices at P5 after administration at E12.5. Quantification is shown in (**c**). No statistically significant differences were observed between control and mutant neurons in regions without ectopia. (**d-f**) BrdU staining in control (**d**) and mutant (**e**) cortices at P5 after administration at E15.5. Quantification is shown in (**f**). Neuronal migration appears slightly delayed in mutants as compared to controls. *, $P<0.05$; **, $P<0.01$; n=5.

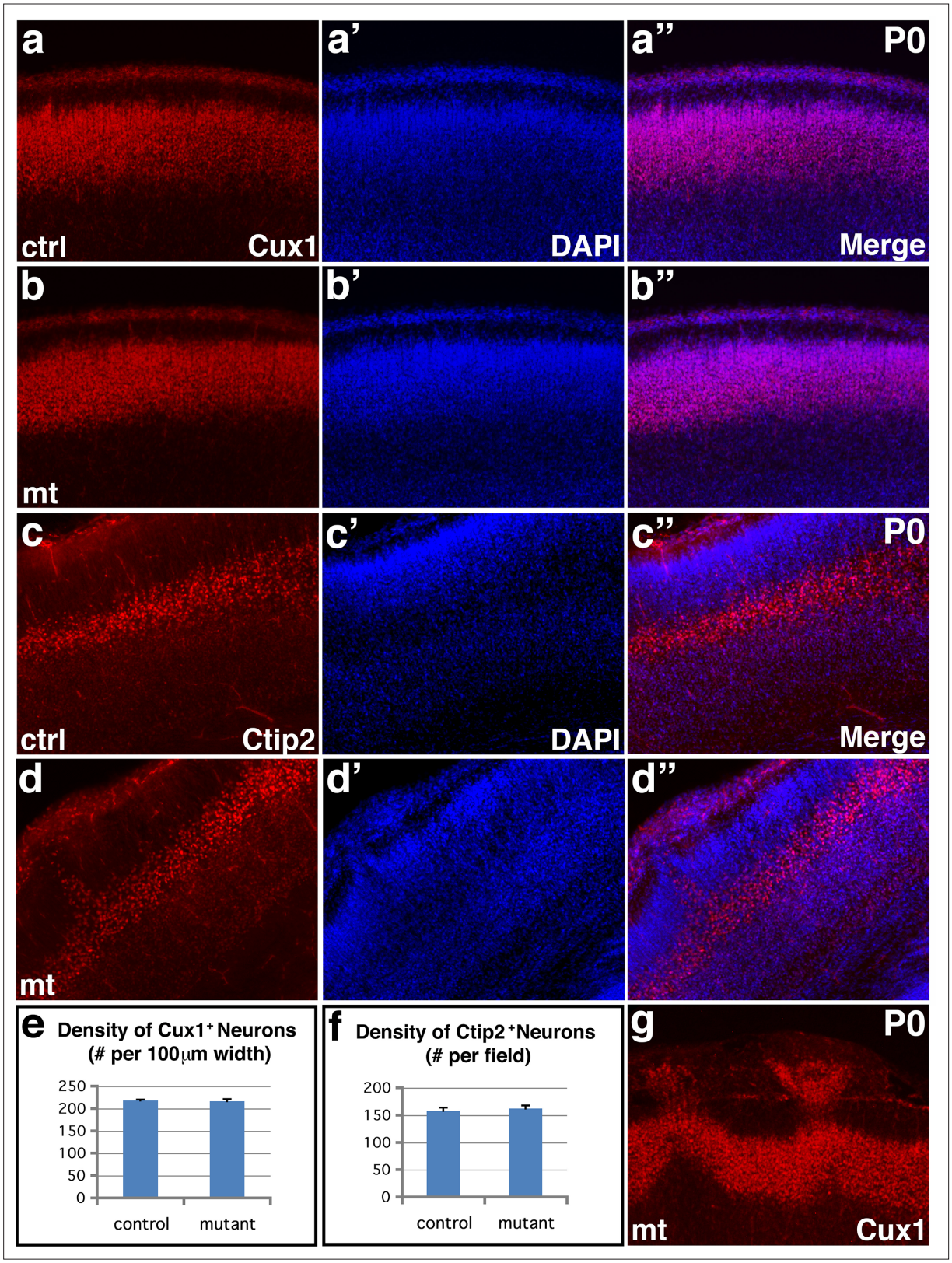

Figure 1—figure supplement 2. Lamina-specific neuronal markers are normal outside ectopia in *Ric8a:Emx1-Cre* mutant cortices. (**a–b**)(**"**) Cux1 (in red) and nuclear (DAPI, in blue) staining of control (**a-a"**) and mutant (**b-b"**) cortices at P0 in a region without ectopia. No obvious changes in the expression pattern of Cux1, an upper layer neuronal marker, were observed in the mutant cortex, except in areas with ectopia (see panel (**g**)). (**c-d"**) Ctip2 (in red) and nuclear (DAPI, in blue) staining of control (**c-c"**) and mutant (**d-d"**) cortices at P0. No obvious changes in the expression pattern of Ctip2, a deep

Figure 1—figure supplement 2 continued on next page

Figure 1—figure supplement 2 continued

layer neuronal marker, were observed in the mutant cortex, except in areas with ectopia. (**e–f**) Quantification of cortical neurons positive for Cux1 (**e**) and Ctip2 (**f**) in matching cortical regions at P0. No significant differences were observed in the density of Cux1 (control, 218.1±1.7 per 100 μm cortical width; mutant, 216.4±4.3 per 100 μm cortical width; *P*=0.36, n=12) or Ctip2 (control, 157.8±5.0 per field; mutant, 161.9±5.9 per field; *P*=0.31, n=12) positive neurons between controls and mutants. (**g**) Cux1 (in red) staining of mutant cortices at P0 in a region with ectopia. Scale bar in (**a**), 200 μm for all panels.

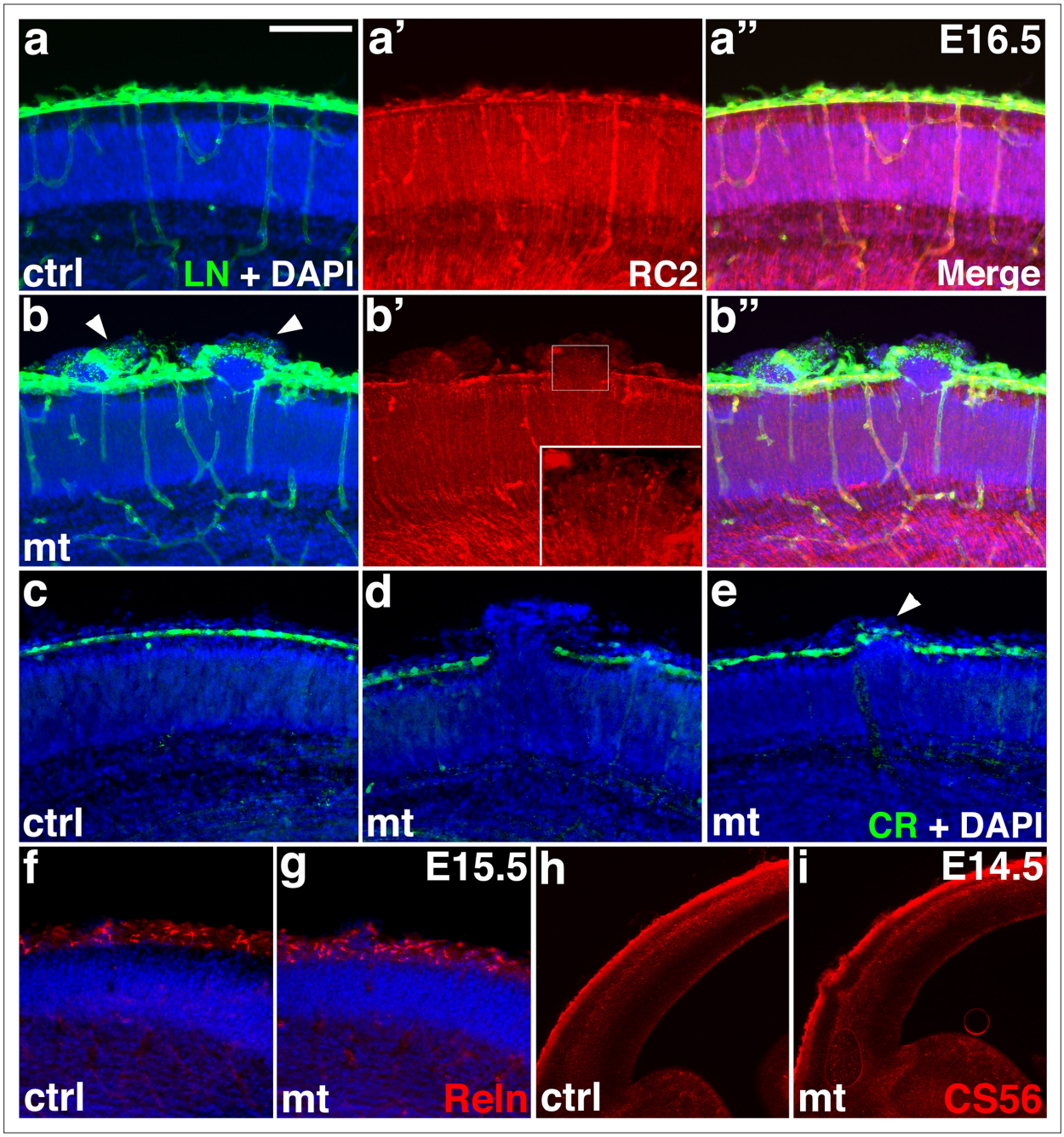

Figure 1—figure supplement 3. Neuronal ectopia in *Ric8a:Emx1-Cre* mutants result from pial basement membrane breach during embryogenesis. (**a-a''**) Laminin (LN, in green), radial glial marker RC2 (in red), and nuclear (DAPI, in blue) staining of control cortices at E16.5. A continuous basement membrane is observed at the pia, where radial glial endfeet are anchored. (**b-b''**) Laminin, RC2, and nuclear staining of *Ric8a:Emx1-Cre* mutant cortices at E16.5. Neuronal ectopias are consistently observed at sites of basement membrane breakage (arrowheads in **b**). Radial glial fibers at these sites extend beyond the pia (inset in **b'**). (**c–e**) Calretinin (CR, in green) and nuclear (DAPI, in blue) staining of control (**c**) and mutant (**d-e**) cortices at E16.5. A continuous row of Calretinin positive Cajal-Retzius cells is observed in the marginal zone of control cortices (**c**). By contrast, in mutants, Cajal-Retzius cells are absent at large ectopias (**d**). However, they appear passively displaced by over-migrating neurons at small ectopias (arrowhead in **e**). (**f–g**) Reelin (Reln, in red) and nuclear (DAPI, in blue) staining of control (**f**) and *Ric8a:Emx1-Cre* mutant (**g**) cortices at E15.5. Strong Reelin expression is observed in Cajal-Retzius cells in the marginal zone of both control and mutant cortices. (**h–i**) Chondroitin sulfate proteoglycan (CS56, in red) staining of control (**h**) and mutant (**i**) cortices at E14.5. Normal preplate splitting is observed in mutants. Scale bar in (**a**), 200 μm for (**a–g**) and 500 μm for (**h–i**).

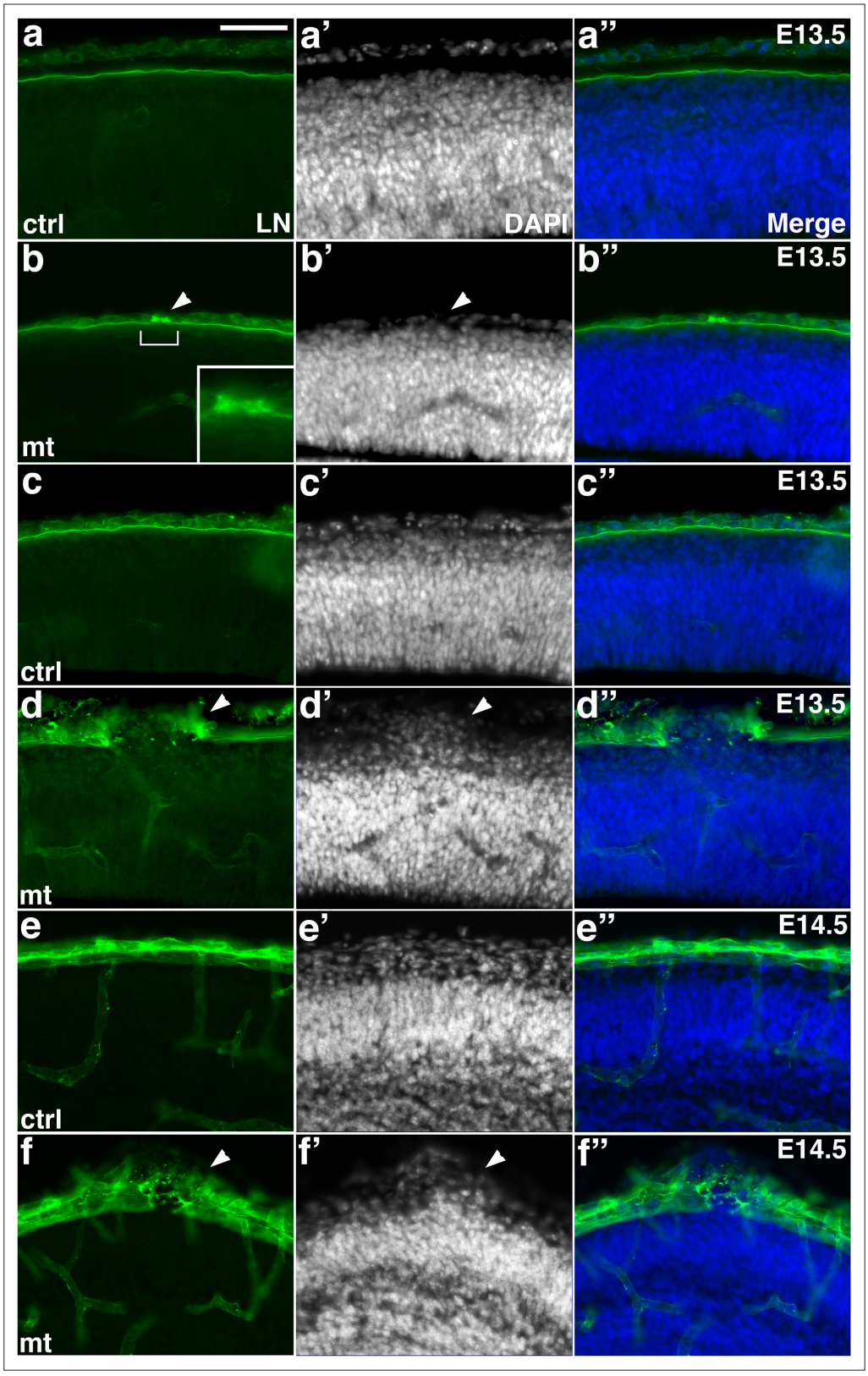

Figure 1—figure supplement 4. Basement membrane breaches precede neuronal ectopia in *Ric8a:Emx1-Cre* mutant cortice. s. (**a-a''**) Laminin (LN, in green) and nuclear (DAPI, in blue) staining of control cortices at E13.5. A continuous basement membrane is observed at the pia, beneath which cells are well organized in the cortical wall. (**b-b''**) Laminin and nuclear staining of *Ric8a:Emx1-Cre* mutant cortices at E13.5. In a subset of mutants, a

Figure 1—figure supplement 4 continued on next page

Figure 1—figure supplement 4 continued

small disruption of basement membrane is observed (bracket and inset in **b**), but not yet associated with ectopia (arrowhead in **b'**). (**c-c"**) Laminin (LN, in green) and nuclear (DAPI, in blue) staining of control cortices at E13.5. (**d-d"**) Laminin and nuclear staining of *Ric8a:Emx1-Cre* mutant cortices at E13.5. Although at E13.5 we observe basement membrane defects in the absence of neuronal ectopia (see **b-b"**), when there are neuronal ectopia, they are always associated with basement membrane breakage. (**e-e"**) Laminin and nuclear staining of control cortices at E14.5. (**f-f"**) Laminin and nuclear staining of *Ric8a:Emx1-Cre* mutant cortices at E14.5. Neuronal ectopia at E14.5 are also always associated with basement membrane breakage. Scale bar in (**a**), 100 μm for all panels.

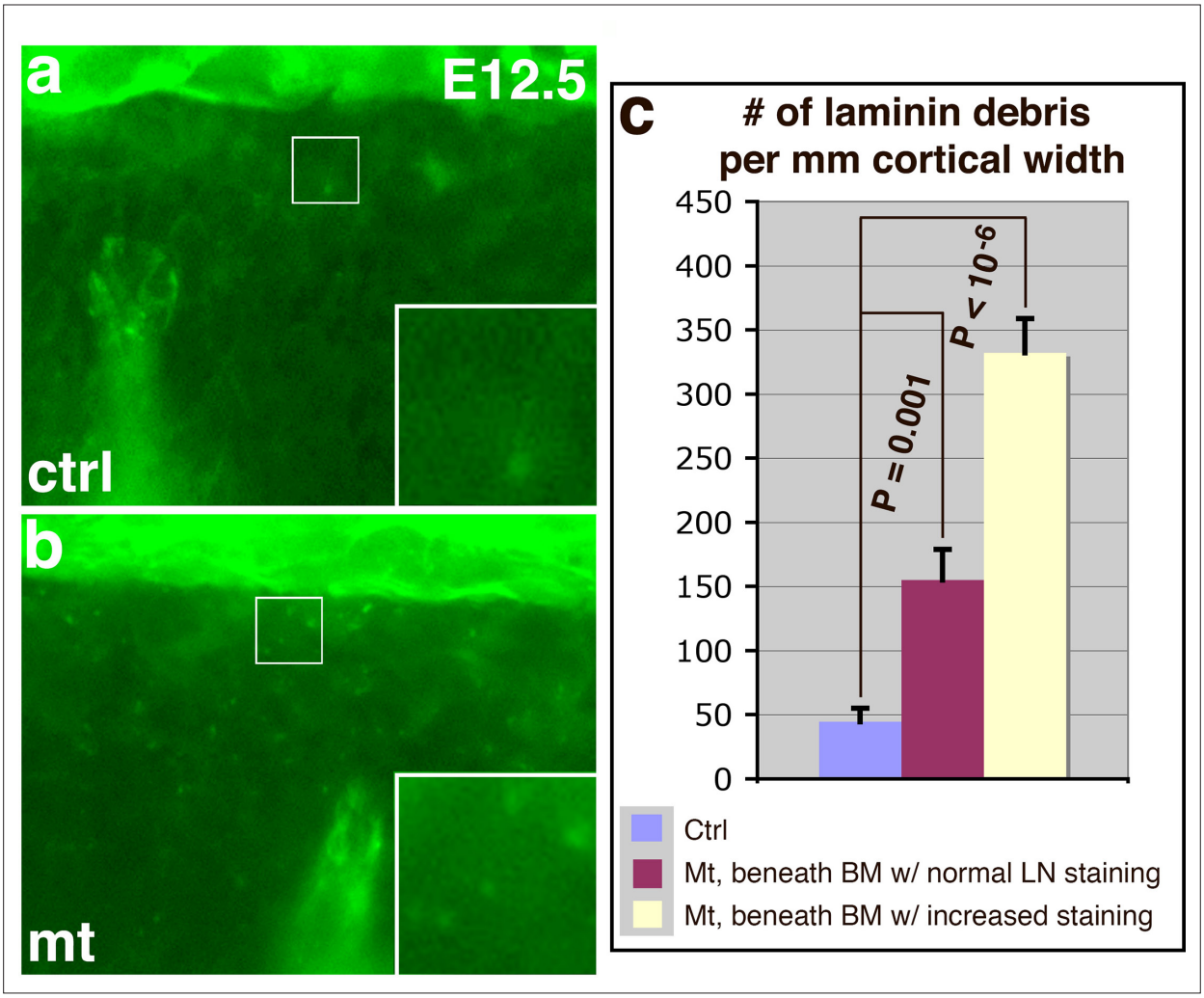

Figure 1—figure supplement 5. Signs of basement membrane degradation before breach formation at E12.5. (**a–b**) Laminin (in green) staining of control (**a**) and *Ric8a:Emx1-Cre* mutant (**b**) cortices at E12.5. Increased numbers of laminin positive debris were observed in mutants (compare insets), even though breaches had yet to form. (**c**) Quantitative analysis shows significant increases.

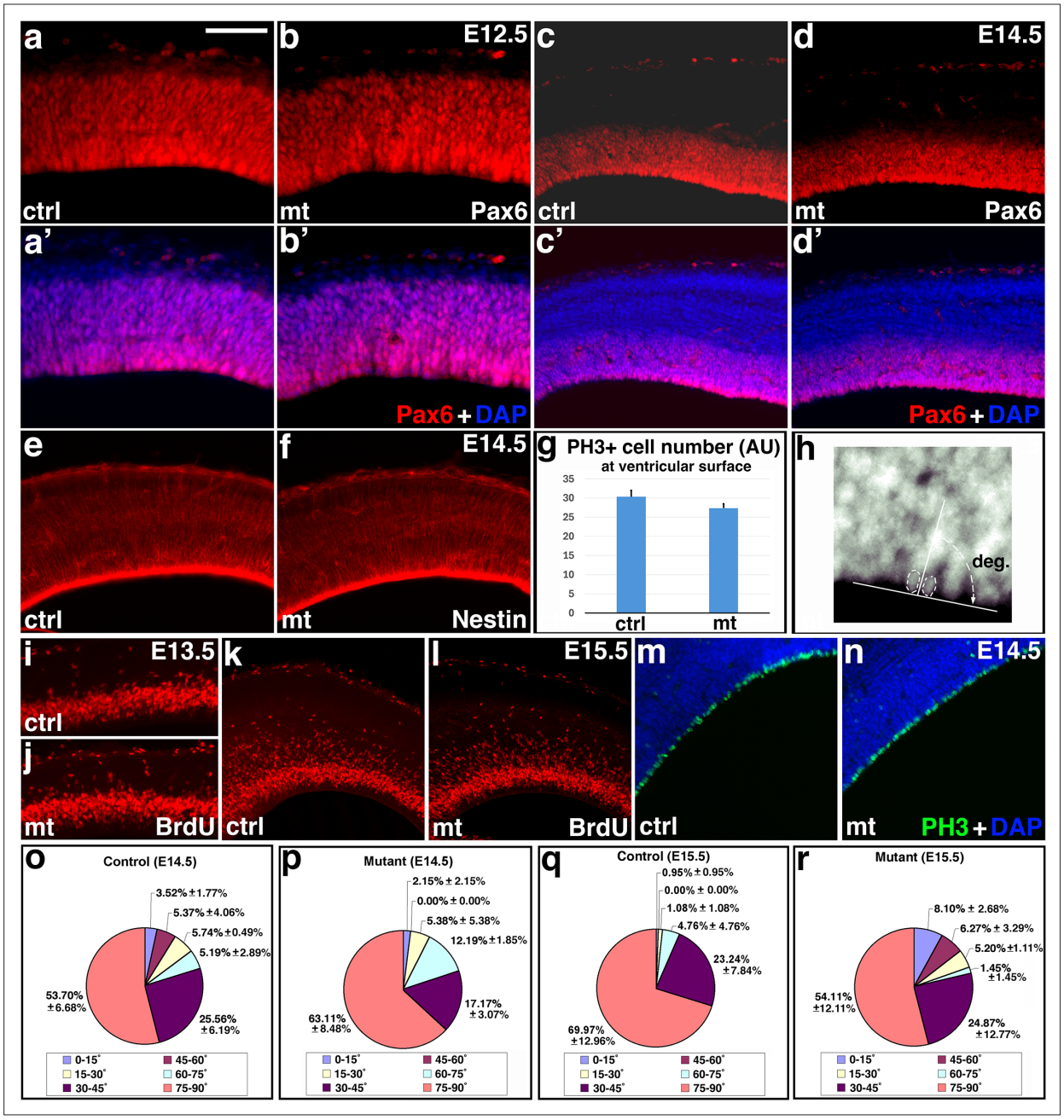

Figure 1—figure supplement 6. Cortical radial glial identity and proliferation are unaffected in *Ric8a:Emx1-Cre* mutants. (**a-b'**) Pax6 (in red) and nuclear (DAPI, in blue) staining of control (**a**&**a'**) and mutant (**b**&**b**) cortices at E12.5. (**c-d'**) Pax6 (in red) and nuclear (DAPI, in blue) staining of control (**c**&**c'**) and mutant (**d**&**d'**) cortices at E14.5. No ectopic Pax6 positive cells were observed at either E12.5 or E14.5. (**e–f**) Nestin (in red) and nuclear (DAPI, in blue) staining of control (**e**) and mutant (**f**) cortices at E14.5. (**g**) Quantification showed no significant differences in the number of phospho-histone 3 (PH3) positive cells at the ventricular surface between control and mutants at E14.5 (AU, arbitrary units; *P*=0.15, n=9 each). See also images in (**m–n**). (**h**) Cleavage plane of neural progenitors is defined by the angle between the equatorial plate and the ventricular surface. See quantification results in (**o–r**). (**i–j**) BrdU staining (in red) in control (**i**) and mutant (**j**) cortices at E13.5. (**k–l**) BrdU staining (in red) in control (**k**) and mutant (**l**) cortices at E15.5. (**m–n**) Phospho-histone 3 (PH3, in green) and nuclear (DAPI, in blue) staining of control (**m**) and mutant (**n**) cortices at E14.5. (**o–p**) Cleavage plane distribution of radial glial mitosis in control (**o**) and mutant (**p**) cortices at E14.5. No significant differences were observed (*P*>0.4, n=3 animals each genotype; 73 cells for controls and 76 cells for mutants). (**q–r**) Cleavage plane distribution of radial glial mitosis in control (**q**) and mutant (**r**) cortices at E15.5. No significant differences were observed (*P*>0.1, n=3 animals each genotype; 70 cells for controls and 59 cells for mutants). Scale bar in (**a**), 100 μm for (**a-b'**) and 200 μm for (**c–n**).

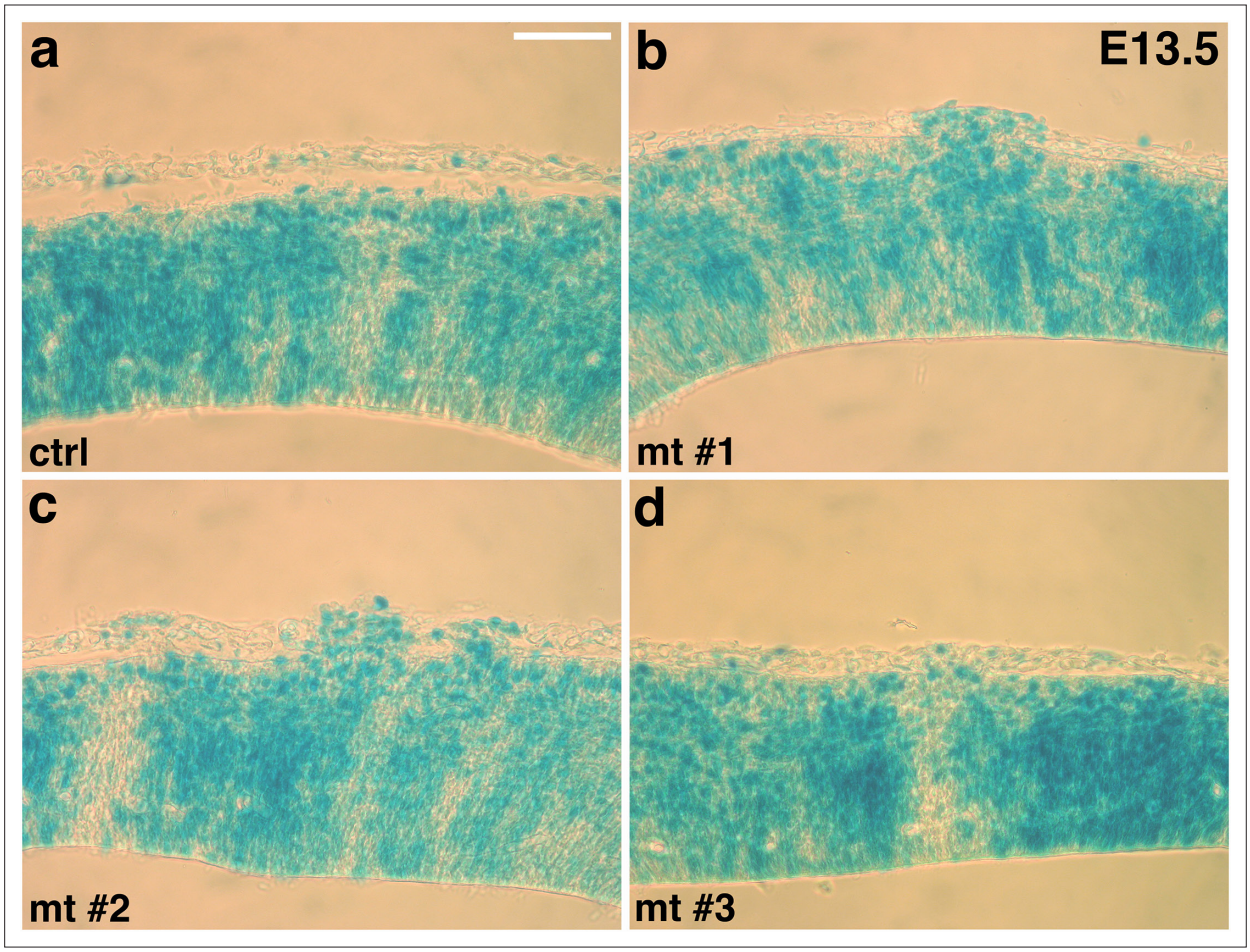

Figure 1—figure supplement 7. Wnt pathway activity is normal in *Ric8a:Emx1-Cre* mutant cortices. X-gal staining of BAT-lacZ expression in *Ric8a:Emx1-Cre* control (**a**) and mutant (**b–d**) cortices at E13.5. No obvious differences are observed between controls and three different mutants at this stage.

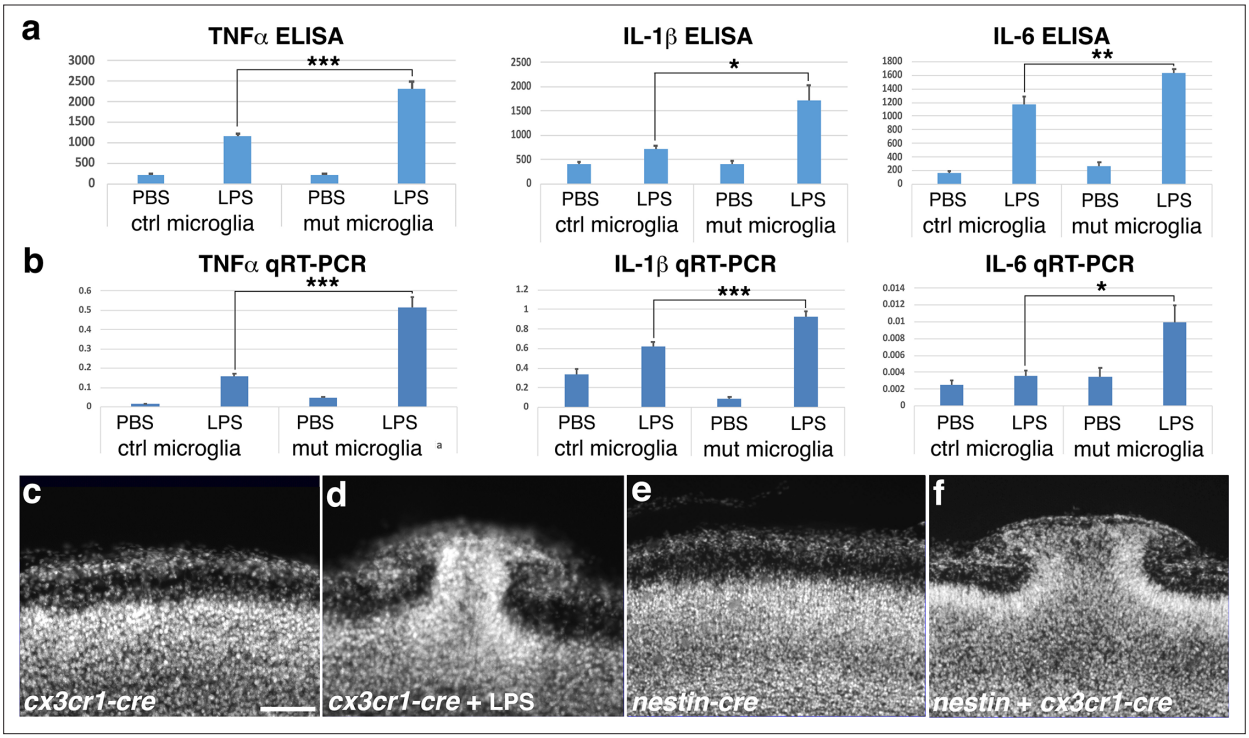

Figure 2. *Ric8a* deficiency in microglia is responsible for cortical ectopia. (**a**) TNFα, IL-1β, and IL-6 secretion (pg/ml) in control and *Ric8a:Cx3cr1-Cre* mutant microglia following LPS stimulation. *, *P*<0.05; **, *P*<0.01; ***, *P*<0.001; n=6–8 each group. (**b**) TNFα, IL-1β, and IL-6 mRNA expression in control and *Ric8a:Cx3cr1-Cre* mutant microglia following LPS stimulation. *, *P*<0.05; ***, *P*<0.001; n=5–6 each group. (**c–d**) Nuclear (DAPI, in grey) staining of *Ric8a:Cx3cr1-Cre* mutant cortices at P0 in the absence (**c**) or presence (**d**) of LPS treatment during embryogenesis. (**e–f**) Nuclear (DAPI, in grey) staining of *Ric8a:Nestin-Cre* single *cre* (**e**) and *Ric8a:Nestin-Cr +Cx3cr1-Cre* double *Cre* (**f**) mutant cortices at P0. Scale bar in (**c**), 100 μm for (**c–f**).

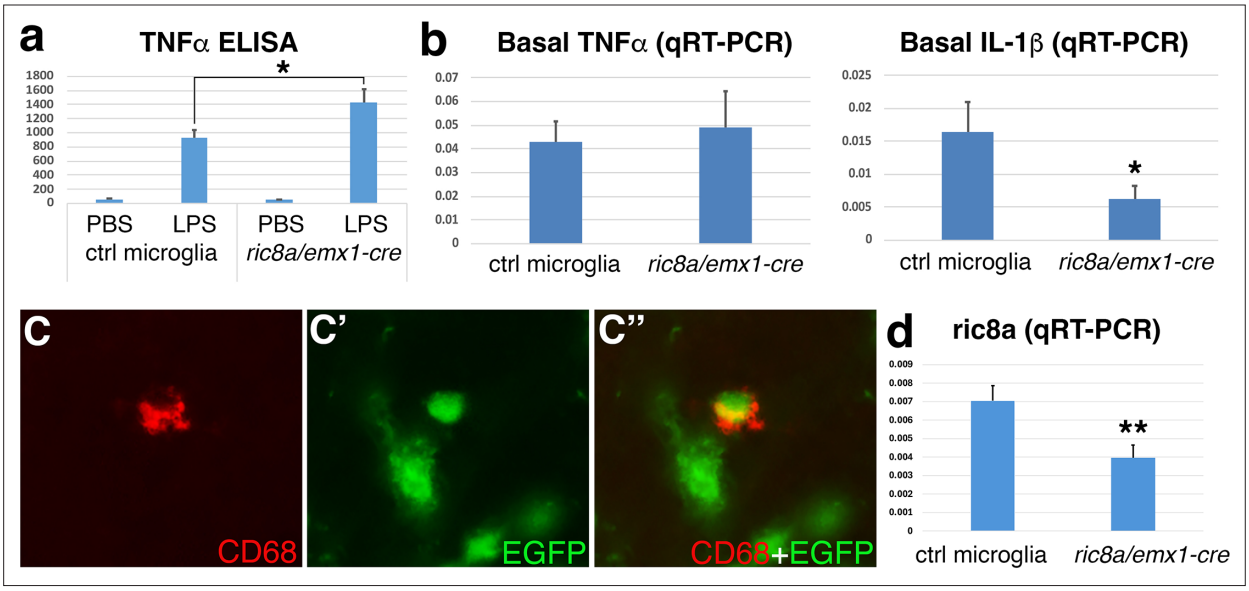

Figure 2—figure supplement 1. *Emx1-Cre* is active in microglia. (**a–b**) TNFα secretion (pg/ml) (**a**) and basal TNFα and IL-1β mRNA expression (**b**) in control and *Ric8a:Emx1-Cre* mutant microglia. *, *P*<0.05; n=5–8 each group. (**c-c''**) The Rosa26 EGFP (green) is induced in CD68 positive (red) microglial cells by *Emx1-Cre*. (**d**) Quantitative RT-PCR analysis of microglia cultured from *Ric8a:Emx1-Cre* mutant cortices showed severe loss of *Ric8a* mRNA in microglial cells. **, *P*<0.01; n=5–8 each group.

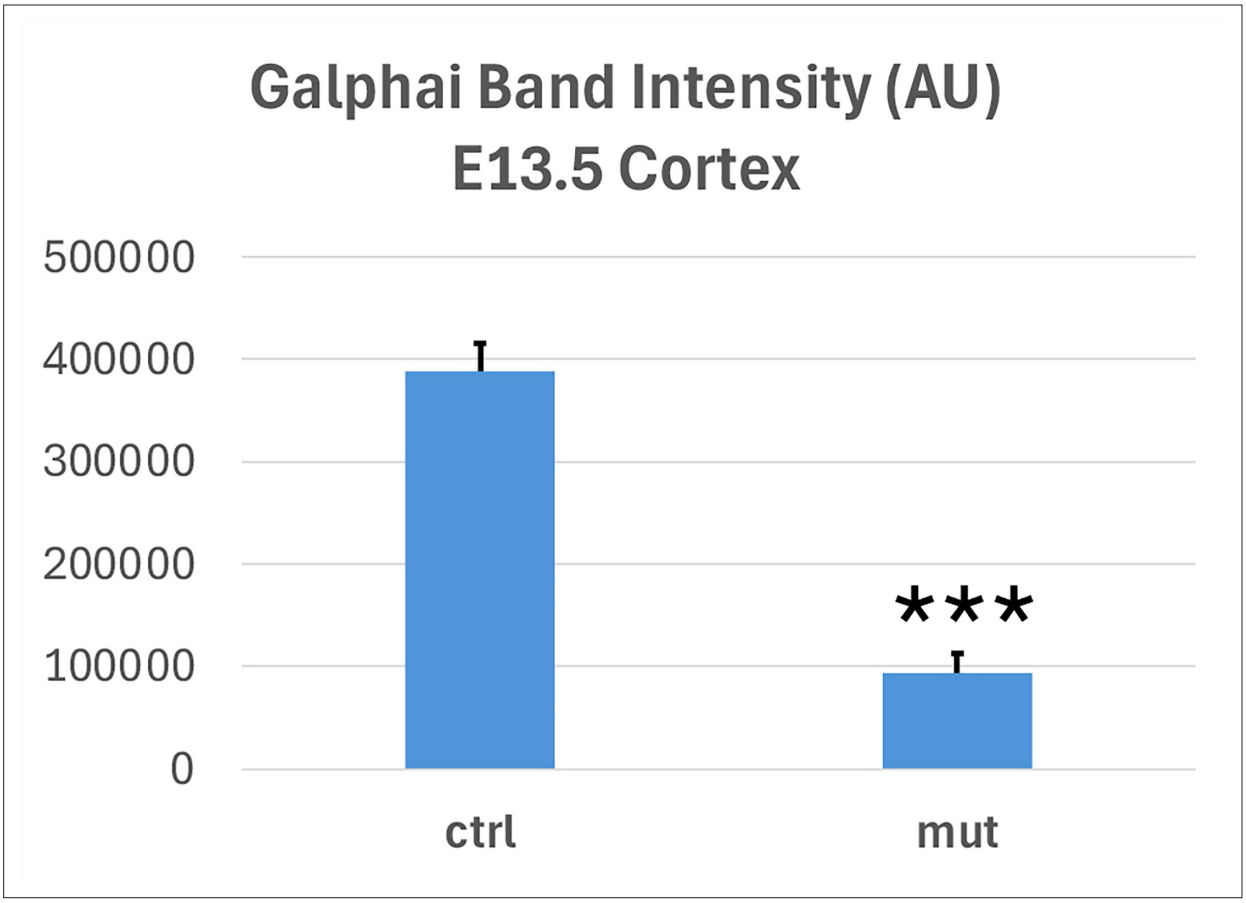

Figure 2—figure supplement 2. Gαi protein is severely depleted from *Ric8a:Emx1-Cre* mutant cortices. Western blot analysis of Gai proteins in E13.5 *Ric8a:Emx1-Cre* mutant cortices showed that Gαi protein levels were severely reduced (AU, arbitrary units). *P*<0.001, n=3 each.

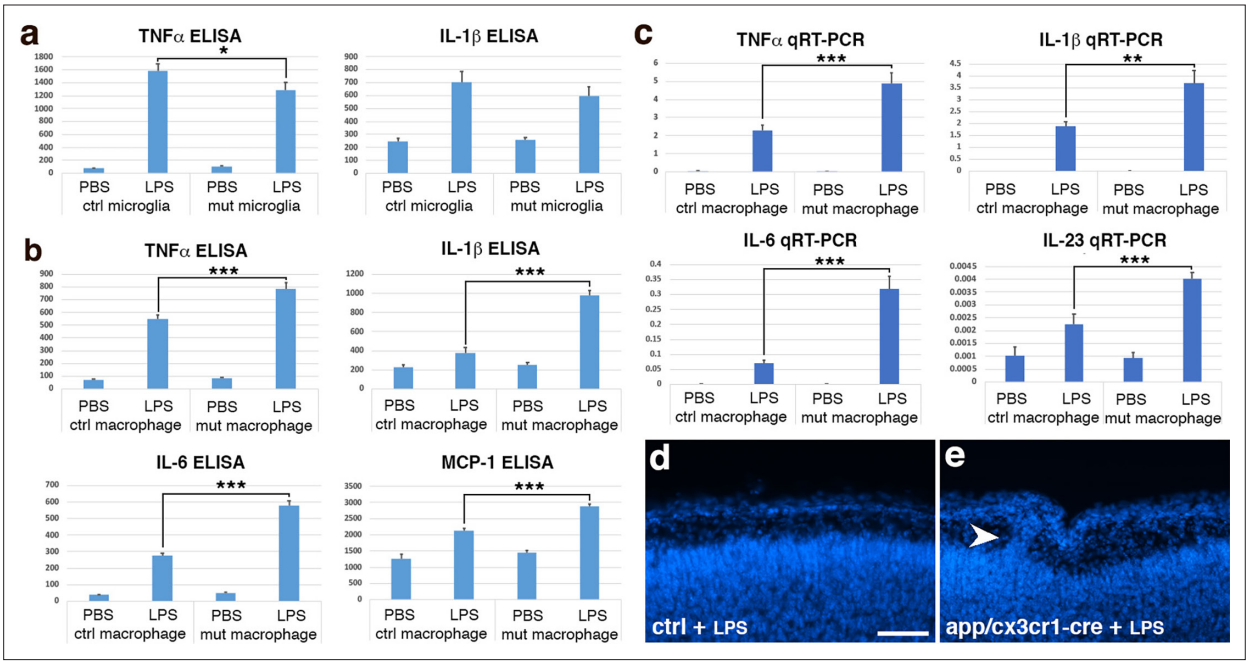

Figure 3. *App* deficiency results in hypersensitive microglia and cortical ectopia. (**a**) TNFα and IL-1β secretion (pg/ml) in cultured control and *App:Cx3cr1-Cre* mutant microglia following LPS stimulation. *, *P*<0.05; n=7–9 each group. (**b**) TNFα, IL-1β, IL-6, and MCP1 secretion (pg/ml) in fresh unelicited control and *App:Cx3cr1-Cre* mutant peritoneal macrophages following LPS stimulation. ***, *P*<0.001; n=7–10 each group. (**c**) TNFα, IL-1β, IL-6, and IL-23 mRNA expression in fresh unelicited control and *App:Cx3cr1-Cre* mutant peritoneal macrophages following LPS stimulation. **, *P*<0.01; ***, *P*<0.001; n=6 each group. (**d-e**) Nuclear (DAPI, in blue) staining of control (**D**) and LPS-treated *App:Cx3cr1-Cre* mutant (**E**) cortices at P0. Note cortical ectopia in the mutant cortex (arrowhead). Scale bar in (**d**), 200 μm for (**d-e**).

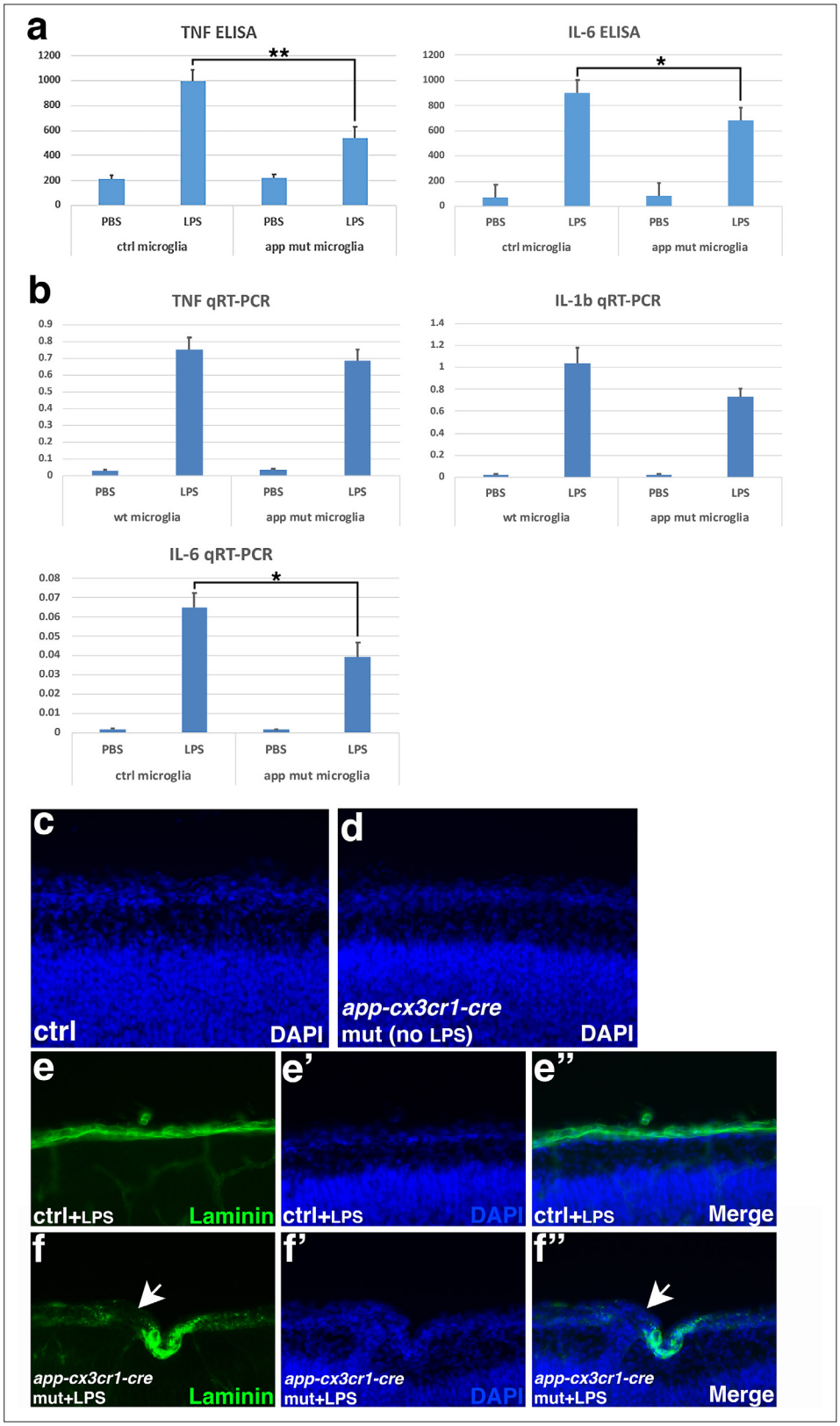

Figure 3—figure supplement 1. Cytokine secretion and transcriptional induction in *App:Cx3cr1-Cre* mutant microgli. a. (**a**) TNFα and IL-6 secretion (pg/ml) in control and *App:Cx3cr1-Cre* mutant microglia following overnight LPS stimulation. *, *P*<0.05; **, *P*<0.01; n=9–13 each group. (**b**) TNFα, IL-1β and IL-6 mRNA expression in control and *App:Cx3cr1-Cre* mutant microglia following overnight 3 hr LPS stimulation. *, *P*<0.05; n=6–7 each

Figure 3—figure supplement 1 continued on next page

Figure 3—figure supplement 1 continued

group. (**c–d**) *App:Cx3cr1-Cre* mutant cortices showed no ectopia at P0 without LPS treatment at embryonic stages (DAPI, blue). (**e-f″**) *App:Cx3cr1-Cre* mutant cortices treated with LPS at embryonic stages showed perturbed basement membrane and gaps at sites of ectopia (white arrows) at P0 (Laminin, green; DAPI, blue).

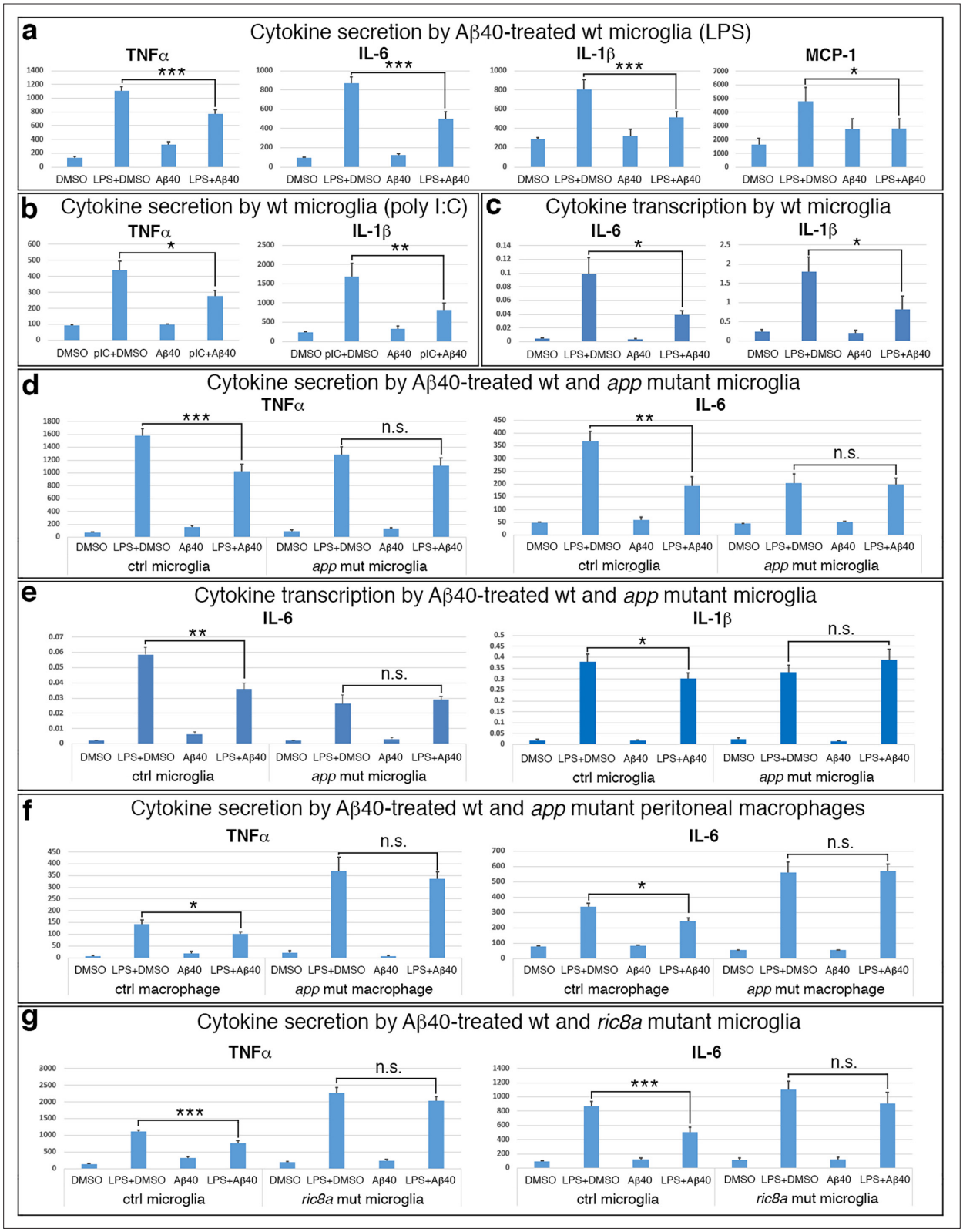

Figure 4. Monomeric Aβ40 suppresses microglia via APP and Ric8a. (**a**) TNFα, IL-6, IL-1β, and MCP1 secretion (pg/ml) by wildtype microglia following LPS stimulation in the absence or presence of Aβ40 (200 or 500 nM). *, $P<0.05$; ***, $P<0.001$; n=8–14 each group. (**b**) TNFαand IL-1β secretion (pg/ml) by wildtype microglia following poly I:C stimulation in the absence or presence of Aβ40 (500 nM). *, $P<0.05$; **, $P<0.01$; n=6–7 each group. (**c**) IL-6 and IL-1β mRNA induction in wildtype microglia following LPS stimulation in the absence or presence of Aβ40 (500 nM). *, $P<0.05$; n=6 each group. (**d**) TNFα

Figure 4 continued on next page

Figure 4 continued

and IL-6 secretion (pg/ml) by control and *App:Cx3cr1-Cre* mutant microglia following LPS stimulation in the absence or presence of Aβ40 (200 nM). **, $P<0.01$; ***, $P<0.001$; n=8 each group. (**e**) IL-6 and IL-1β mRNA induction in control and *App:Cx3cr1-Cre* mutant microglia following LPS stimulation in the absence or presence of Aβ40 (200 nM). *, $P<0.05$; **, $P<0.01$; n=6 each group. (**f**) TNFαand IL-6 secretion (pg/ml) by control and *App:Cx3cr1-Cre* mutant peritoneal macrophages following LPS stimulation in the absence or presence of Aβ40 (500 nM). *, $P<0.05$; n=6–7 each group. (**g**) TNFα and IL-6 secretion (pg/ml) by control and *Ric8a:Cx3cr1-Cre* mutant microglia following LPS stimulation in the absence or presence of Aβ40 (200 nM). ***, $P<0.001$; n=12–14 each group.

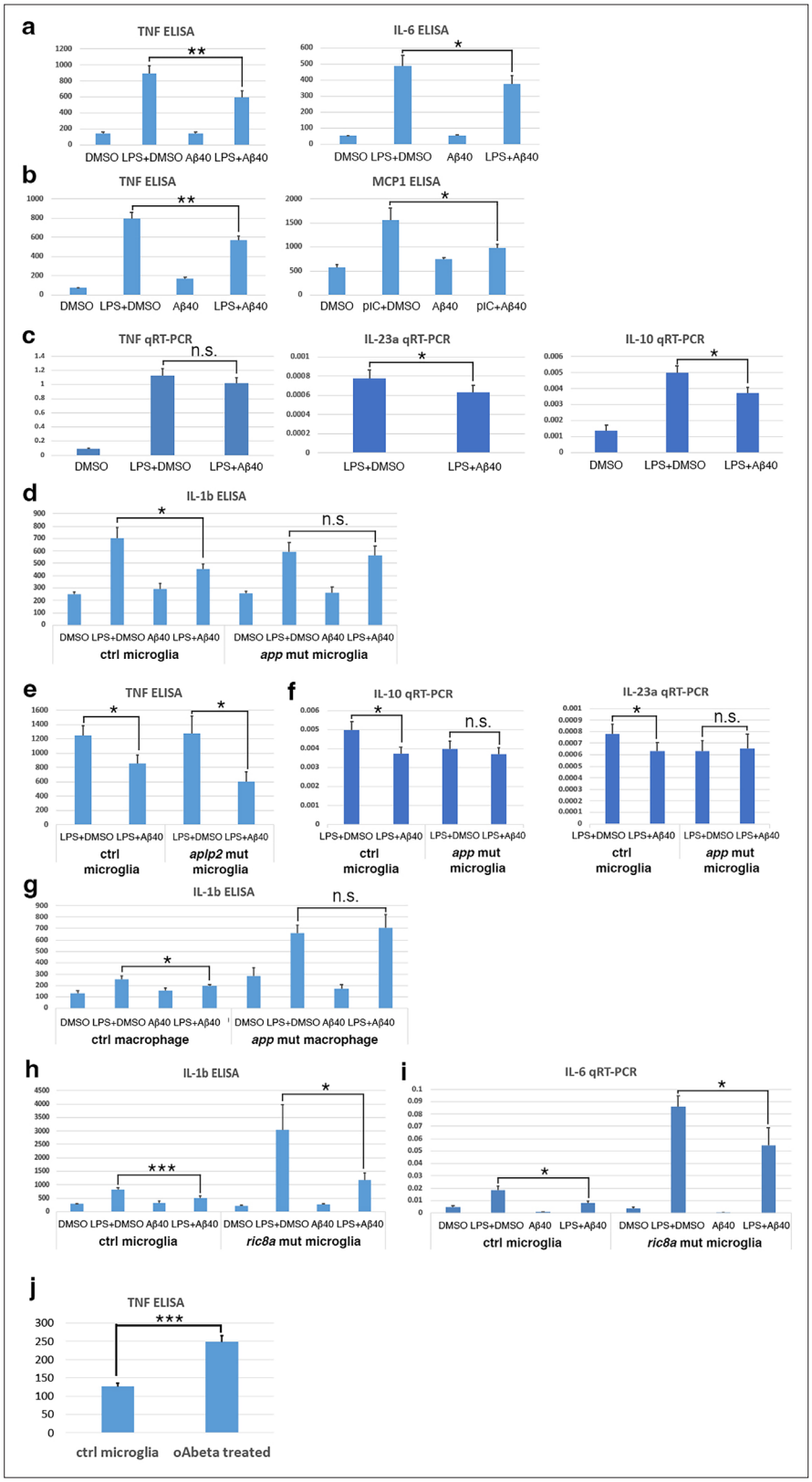

Figure 4—figure supplement 1. Effects of monomeric Aβ on cytokine secretion and transcription in control and mutant microglial lineage cells. (**a**) TNFα and IL-6 secretion (pg/ml) in wildtype microglia following LPS stimulation in the absence or presence of Aβ40 (50 nM). *, $P<0.05$; **, $P<0.01$; n=25 each group for TNFα and 11 each group for IL-6. (**b**) TNFα and MCP1 secretion (pg/ml) in wildtype microglia following LPS stimulation in the

Figure 4—figure supplement 1 continued on next page

Figure 4—figure supplement 1 continued

absence or presence of Aβ40 (500 nM) from Genscript. Effects on IL-1β secretion in ***Figure 4b*** was also performed with Genscript Aβ40. All other experiments in Fig. 7 were performed with ApexBio Aβ40. *, $P<0.05$; **, $P<0.01$; n=5–7 each group. (**c**) TNFα, IL-23, and IL-10 mRNA expression in wildtype microglia following LPS stimulation in the absence or presence of Aβ40 (400 nM). *, $P<0.05$; n=6 each group. (**d**) IL-1β secretion (pg/ml) in control and *App:Cx3cr1-Cre* mutant microglia following LPS stimulation in the absence or presence of Aβ40. *, $P<0.05$; n=8–12 each group. (**e**) TNFα (pg/ml) in control or *Aplp2:Cx3cr1-Cre* mutant microglia following LPS stimulation in the absence or presence of Aβ40 (400 nM). *, $P<0.05$; n=9–13 each group. (**f**) IL-10 and IL-23 mRNA expression in control and *App:Cx3cr1-Cre* mutant microglia following LPS stimulation in the absence or presence of Aβ40 (400 nM). *, $P<0.05$; n=6 each group. (**g**) IL-1β secretion (pg/ml) in fresh unelicited control and *App:Cx3cr1-Cre* mutant peritoneal macrophages following LPS stimulation in the absence or presence of Aβ40 (400 nM). *, $P<0.05$; n=12 each group. (**h**) IL-1β secretion (pg/ml) in f control and *Ric8a:Cx3cr1-Cre* mutant microglia following LPS stimulation in the absence or presence of Aβ40 (500 nM). *, $P<0.05$; ***, $P<0.001$; n=7–8 each group. (**i**) IL-6 mRNA expression in control and *Ric8a:Cx3cr1-Cre* mutant microglia following LPS stimulation in the absence or presence of Aβ40 (200 nM). *, $P<0.05$; n=6 each group. (**j**) TNFα (pg/ml) in wildtype microglia in the absence or presence of Aβ40 oligomers aggregated (at 10 μM monomer equivalent). ***, $P<0.001$; n=10 each group.

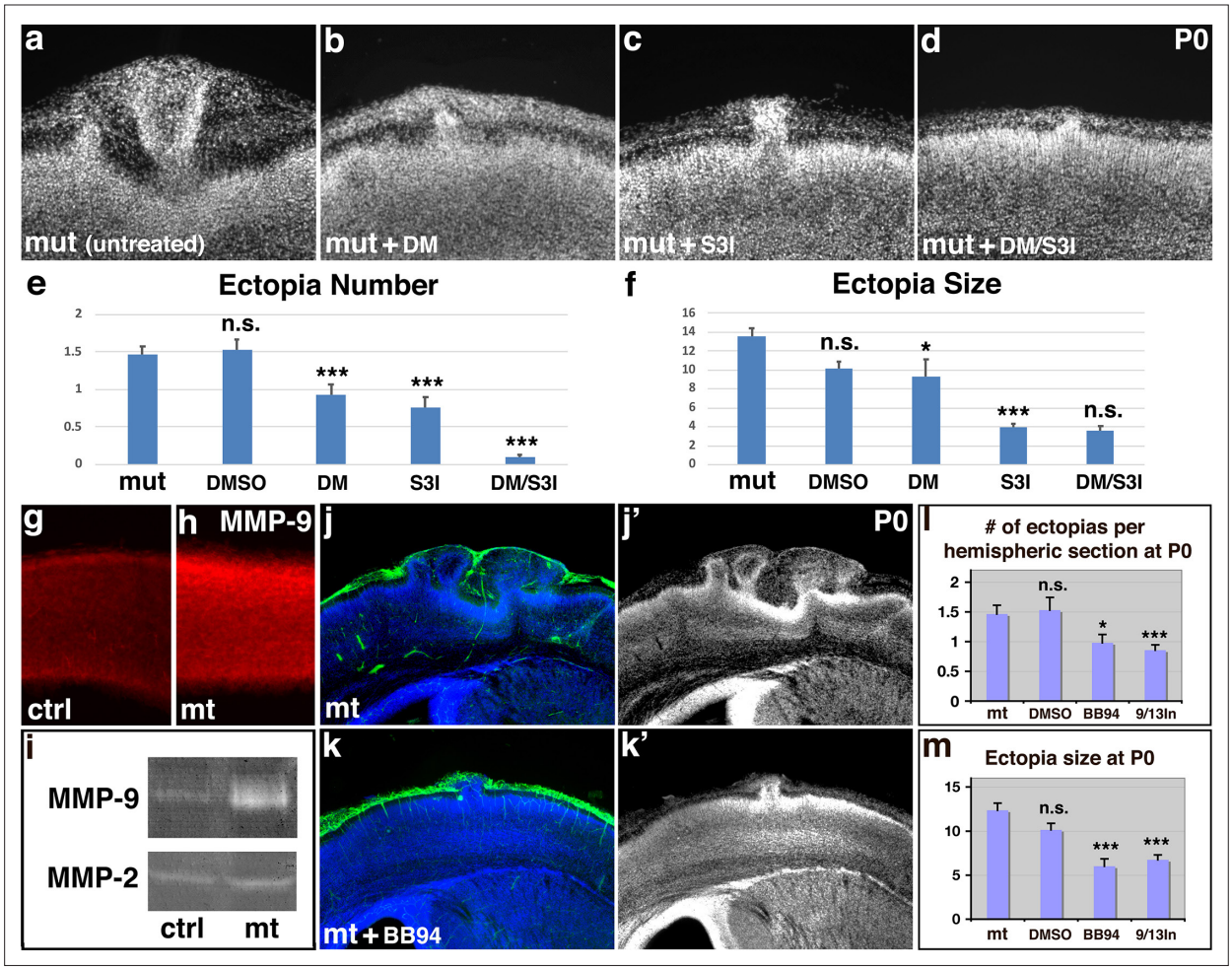

Figure 5. Inhibition of both microglial inflammatory activation and cortical MMP9 activity suppresses basement membrane breach and neuronal ectopia. (**a–d**) Nuclear (DAPI, in grey) staining of untreated (**a**), anti-inflammatory drug dorsomorphin (DM) (**b**), Stat3 inhibitor S3I-201 (S3I) (**c**), and DM/S3I (**d**) dual treated *Ric8a:Emx1-Cre* mutant cortices at P0. (**e–f**) Quantitative analysis of ectopia number (**e**) and size (**f**) in the neonatal mutant cortex after DMSO, DM, S3I, and DM/S3I dual treatment at E12.5. *, *P*<0.05; ***, *P*<0.001; all compared to untreated mutants. The reduction in ectopia size after dual treatment is not statistically significant, likely due to the small number of ectopias that remained. (**g–h**) MMP9 (in red) staining of control (**g**) and mutant cortices (**h**) at E13.5. Quantification shows statistically significant increases in mutants (control, 24.8±0.2 AU (Arbitrary Units); mutant, 35.7±1.7 AU; *P*=0.002; n=6). (**i**) Gel zymography of control and mutant cortical lysates at E13.5. Increased levels of MMP9 but not of MMP2 were observed in mutants (control, 1.00±0.06 AU; mutant, 3.72±1.86 AU; *P*=0.028; n=4). See further details in supplemental Fig. 13. (**j-k'**) Laminin (in green) and nuclear (DAPI, in blue) staining of mutant cortices untreated (**H**) or treated (**I**) with BB94. (**l-m**) Quantitative analysis of ectopia number and size following MMP inhibitor BB94 or MMP9/13 inhibitor I treatment. *, *P*<0.05; ***, *P*<0.001; all compared to untreated mutants.

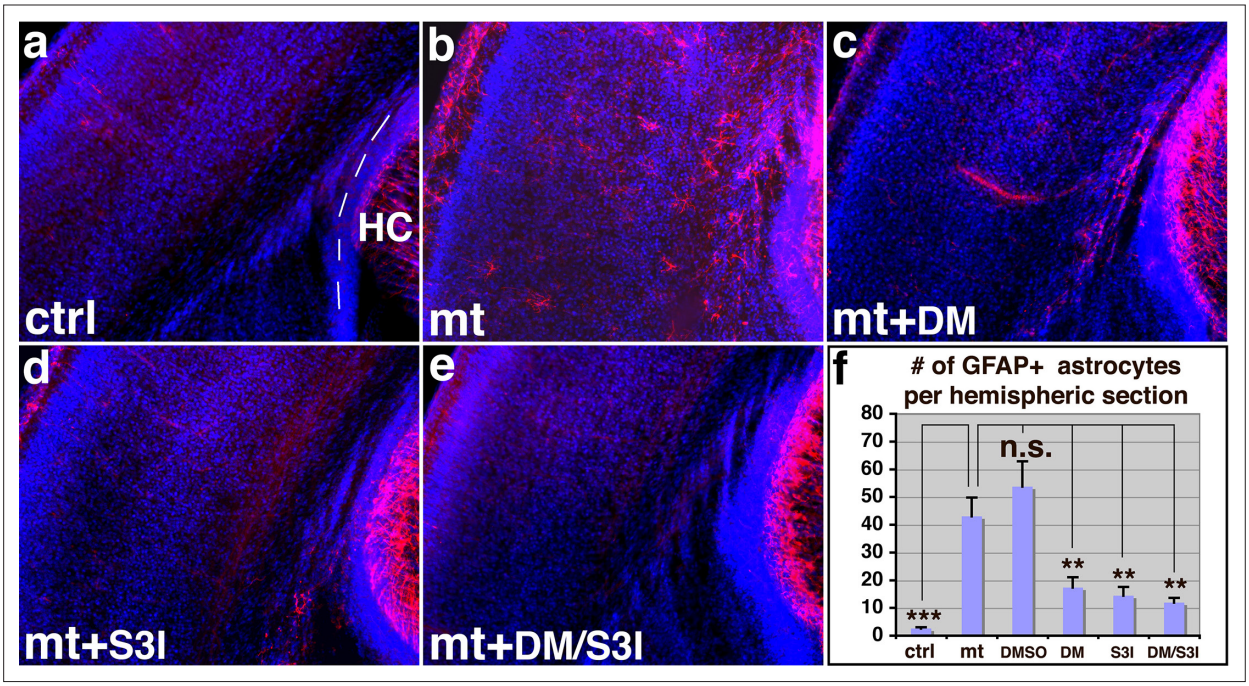

Figure 5—figure supplement 1. Suppression of astrogliosis in *Ric8a:Emx1-Cre* mutant cortices by anti-inflammatory drugs, dorsomorphin (DM) and S3I-201 (S3I). (**a–e**) GFAP (in red) and nuclear (DAPI, in blue) staining of neonatal control (**a**) and mutant cortices without treatment (**b**) or mutant cortices after dorsomorphin DM, (**c**), S3I-201 S3I, (**d**), or dual DM +S3 I, (**e**) treatment at E12.5. Note, GFAP is normally expressed in the neonatal hippocampus (HC) (dashed line in **a**). (**f**) Quantitative analysis of GFAP-positive astrocyte numbers in the neonatal mutant cortex after treatment at E12.5.

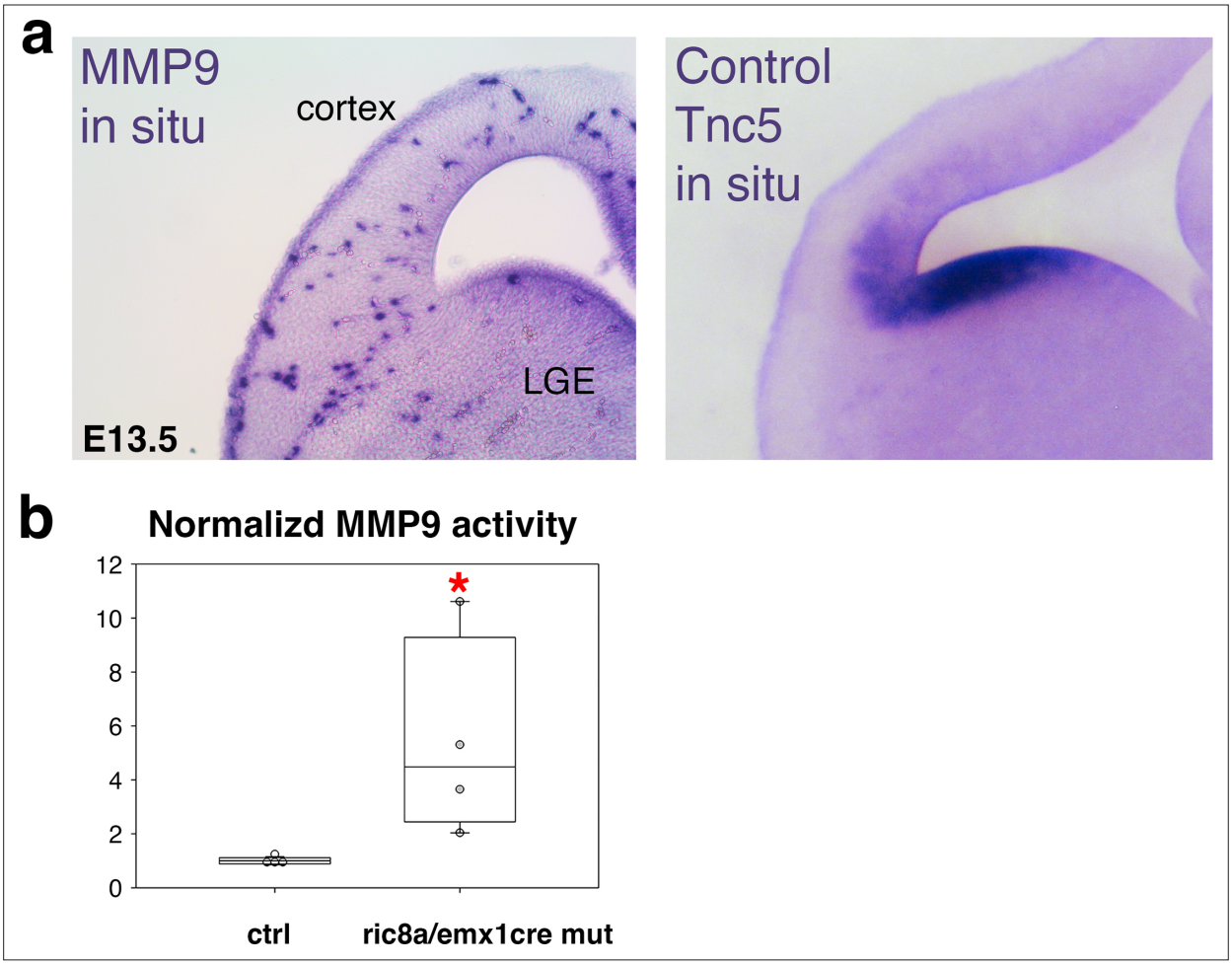

Figure 5—figure supplement 2. MMP9 in situ and activity in E13.5 *Ric8a:Emx1-Cre* mutant cortices. (**a**) Sections of E13.5 brain wholemount in situ of MMP9 showed a sparse MMP9 expressing cell population resembling microglia (LGE, lateral ganglionic eminence). Tnc5 in situ was performed as control for validating probe specificity. (**b**) Quantification showed MMP9 activity levels were significantly increased in E13.5 *, $P<0.05$; n=4 each.

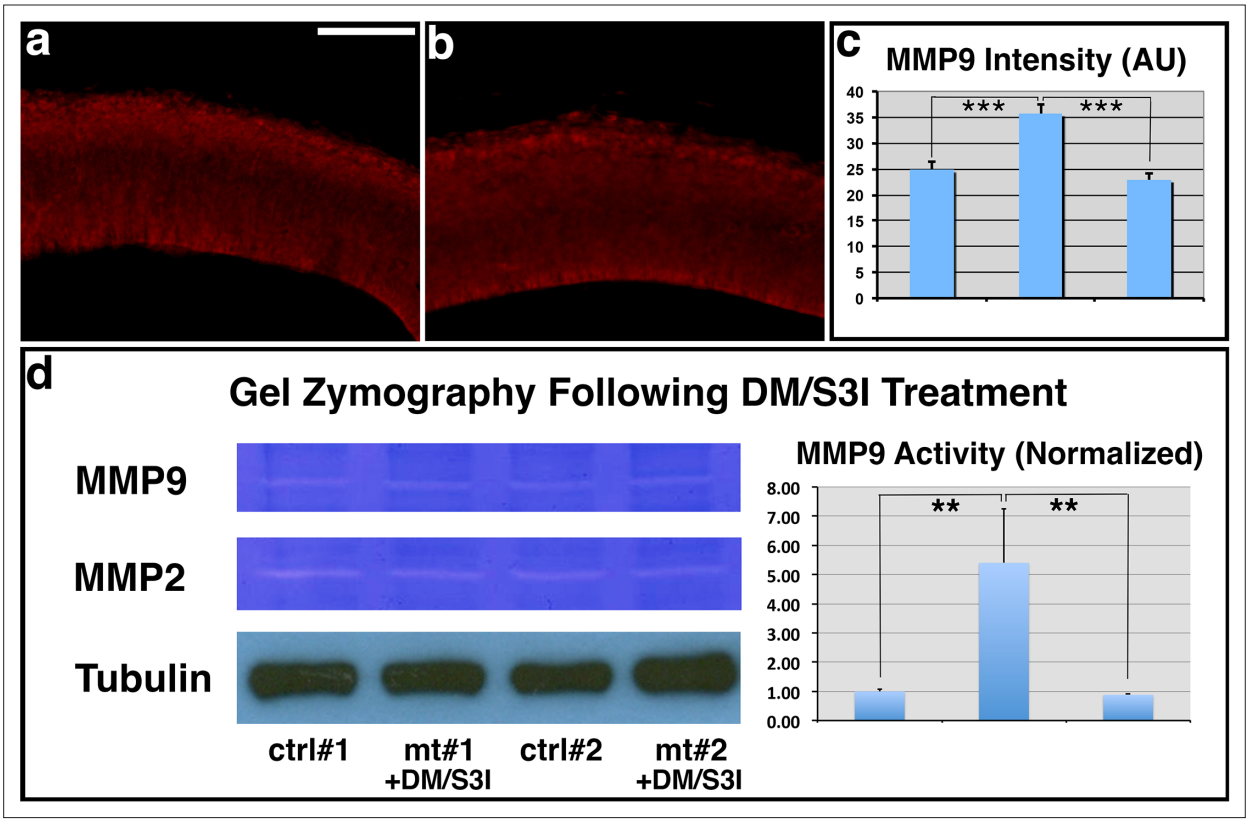

Figure 5—figure supplement 3. Suppression of MMP9 expression in *Ric8a:Emx1-Cre* mutant cortices by anti-inflammatory drugs, dorsomorphin (DM) and S3I-201 (S3I). (**a**) MMP9 (in red) staining in control cortices at E13.5. (**b**) MMP9 (in red) staining in mutant cortices at E13.5 after DM and S3I dual treatment at E12.5. (**c**) Quantitative analysis of MMP9 expression. No significant differences are observed in mutants after inhibitor treatment in comparison to controls (***, $P<0.001$; n=6 each group, ANOVA). (**d**) Gel zymography of E13.5 control and mutant cortical lysates following DM/S3I treatment at E12.5. Similar levels of MMP9 are observed between controls and mutants. Quantification also showed no significant differences in normalized MMP9 levels (**, $P<0.01$; n=4–6 each group, ANOVA).